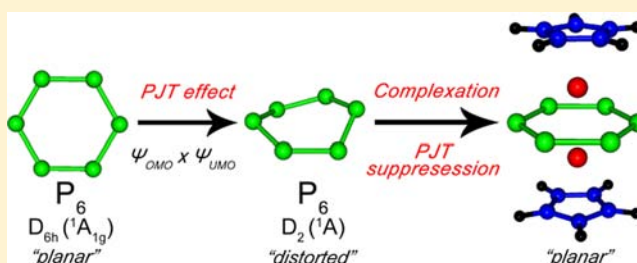


On the Suppression Mechanism of the Pseudo-Jahn–Teller Effect in Middle E_6 ($E = P, As, Sb$) Rings of Triple-Decker Sandwich ComplexesAlexander S. Ivanov,^{†,‡} Konstantin V. Bozhenko,^{*,†} and Alexander I. Boldyrev^{*,‡}[†]Department of Physical and Colloid Chemistry, Peoples' Friendship University of Russia, 6 Miklukho-Maklaya Street, Moscow 117198, Russian Federation[‡]Department of Chemistry and Biochemistry, Utah State University, 0300 Old Main Hill, Logan, Utah 84322, United States

ABSTRACT: Quantum chemical calculations of the $CpMoE_6MoCp$ ($E = P, As, Sb$) triple-decker sandwich complexes showed that E_6 fragments in the central decks of the complexes are planar. Analysis of molecular orbitals involved in vibrational coupling demonstrated that filling the unoccupied molecular orbitals involved in vibronic coupling with electron pairs of Mo atoms suppresses the PJT effect in the $CpMoE_6MoCp$ ($E = P, As, Sb$) sandwich, with the E_6 ring becoming planar (D_{6h}) upon complex formation. The AdNDP analysis revealed that bonding between $C_5H_5^-$ units and Mo atoms has a significant ionic contribution, while bonding between Mo atoms and E_6 fragment becomes appreciably covalent through the δ -type $M \rightarrow L$ back-donation mechanism.



INTRODUCTION

A planar aromatic structure of benzene is by far the most stable isomer for C_6H_6 stoichiometry.^{1–3} One can think that the

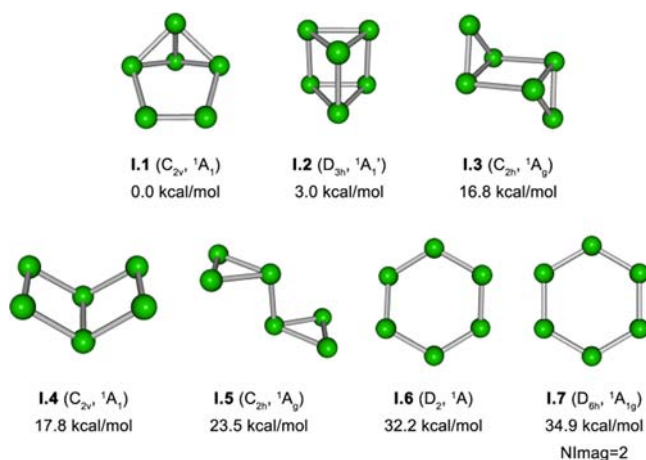


Figure 1. Selected lowest energy structures of P_6 , their point group symmetries, spectroscopic states, and ZPE (B3LYP/6-311+G*) corrected relative energies (CCSD(T)/CBS//B3LYP/6-311+G*).

molecule *cyclo-P₆* (hexaphosphabenzene) being a valence isoelectronic analogue of benzene may have a planar hexagonal structure. In 1985 Scherer et al.⁴ synthesized and characterized the $\{(\eta^5\text{-Me}_5\text{C}_5)\text{Mo}\}_2(\mu,\eta^6\text{-P}_6)$ triple-decker sandwich complex containing a planar P_6 ring with almost equal P–P bonds.⁵ The experimental P–P bond lengths (2.167 and 2.175 Å) are in a good agreement with the theoretical P–P bond (2.125 Å), which is intermediate between typical values for the single P–P

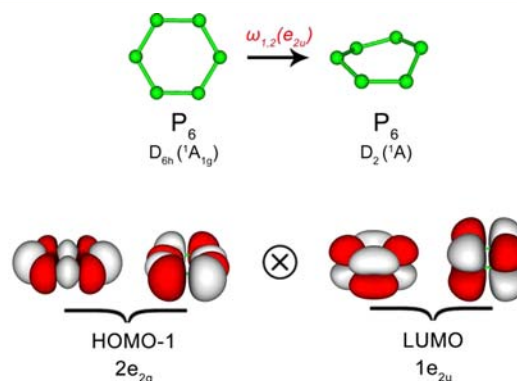


Figure 2. Interaction of the pairs of occupied and unoccupied molecular orbitals of the D_{6h} ($^1A_{1g}$) structure of P_6 responsible for the PJT effect: interactions cause distortion toward the D_2 (1A) structure upon following the doubly degenerate $\omega_{1,2}(e_{2u})$ imaginary frequency mode.

bond of 2.233 Å in P_2H_4 and the double bond 2.044 Å in P_2H_2 (all at MP2/6-31G*⁶). Therefore, the planarity of the P_6 cluster in the triple-decker complex indicates that, indeed, it is aromatic and analogous to benzene. The *cyclo-As₆* planar molecule was also first coordinatively stabilized by Scherer et al.⁷ in 1989 as the central deck of the sandwich complex similar to $\{(\eta^5\text{-Me}_5\text{C}_5)\text{Mo}\}_2(\mu,\eta^6\text{-P}_6)$. The chemical bonding and electronic structure of the metallocenes with P_6 and other aromatic molecules have been thoroughly discussed by Jemmis et al.^{8–10} However, despite the observation of hexagonal

Received: April 16, 2012

Published: July 30, 2012

aromatic hexaphosphabenzene in the triple-decker complex, theoretical calculations revealed^{6,11–20} that there are at least seven nonplanar P_6 isomers lower in energy than the benzene-like D_{6h} structure I.7 (Figure 1).

Moreover, the planar structure I.7 is not a minimum but a second-order saddle point. Geometry optimization following the first imaginary frequency mode of the D_{6h} structure leads to the D_2 -distorted structure I.6, which is 2.7 kcal/mol lower in energy. According to the most accurate calculations,^{6,20} the global minimum structure of P_6 is the benzvalene-like structure I.1 with the prismane-like isomer I.2 being the second lowest and the other isomers lying significantly higher in energy.

Galeev and Boldyrev showed²⁰ that the out-of-plane distortion in P_6 (D_{6h}) is due to the pseudo-Jahn–Teller (PJT) effect.^{21,22} Jahn–Teller vibronic effects were shown by Bersuker^{23–25} to be the only source of instability of high-symmetry configurations of polyatomic systems. The distortion of structure I.7 into structure I.6 occurred due to vibronic coupling of HOMO-1 (e_{2g}) and LUMO (e_{2u}) in P_6 (Figure 2).

The direct product of their symmetries contains e_{2u} , which is the symmetry of the imaginary mode

$$e_{2g} \otimes e_{2u} = a_{1u} \oplus a_{2u} \oplus e_{2u} \quad (1)$$

The symmetry of the imaginary mode (e_{2u}) of the D_{6h} structure corresponds to the totally symmetric (a) mode in the distorted D_2 isomer. Thus, both conditions of the PJT effect (PJTE) are met.²⁰ The HOMO-1 and LUMO gap is 8.29 eV (HF/cc-pVTZ//B3LYP/6-311+G*).¹⁷ The planarization of the P_6 ring in the $\{(\eta^5\text{-Me}_5\text{C}_5)\text{Mo}\}_2(\mu, \eta^6\text{-P}_6)$ complex is due to suppression of the PJT effect. It was shown that the PJTE may be suppressed by increasing the energy gap to the active excited state in the porphyrin ring of hemoglobin via oxygenation and substitution that populates the excited state upon small ligand coordination to hemoproteins.²⁶ Most recently, two more mechanisms for suppression of the PJT effect have been proposed: by the gap increase between the interacting OMO–UMO pair in the external electrostatic field of cations²⁷ and by occupying the interacting UMO with an electron pair upon complexation.²⁸ In this article, we demonstrate that suppression of the PJT effect in the P_6 cluster being the middle deck of the $\{(\eta^5\text{-Me}_5\text{C}_5)\text{Mo}\}_2(\mu, \eta^6\text{-P}_6)$ sandwich complex is due to the second mechanism.

THEORETICAL SECTION

We selected the following neutral complexes $\text{CpMoE}_6\text{MoCp}$ ($E = \text{P, As, Sb}$) as models for our computational analysis of chemical bonding in the experimentally observed triple-decker complex. Geometry optimization and follow-up frequency calculations for the isolated planar E_6 and our model were performed at the hybrid Hartree–Fock/DFT (B3LYP) level of theory.^{29–31} A double- ζ basis set (LanL2DZ)³² for Mo and Sb and standard 6-31G* basis set for other atoms (P, As, C, H) were used.

A chemical bonding analysis of the vibronic coupling was performed at the RHF level of theory using the LanL2DZ basis set for Mo and Sb and 6-31G* basis set for other atoms. Additionally, in order to gain more insight into the structure and chemical bonding of the triple-decker sandwich complexes we performed chemical bonding analysis using the adaptive natural density partitioning (AdNDP) method. The AdNDP developed in our lab by Zubarev and Boldyrev, has been successfully applied for analysis of chemical bonding in boron clusters,³³ prototypical aromatic organic molecules,³⁴ gold clusters,³⁵ and the triple-decker sandwich complex $[\text{Pd}_4(\mu_4\text{-C}_9\text{H}_9)(\mu_4\text{-C}_8\text{H}_8)]\text{-}[\text{BAR}_4^f]$ ($\text{BAR}_4^f = \text{B}\{3,5\text{-}(\text{CF}_3)_2\text{C}_6\text{H}_3\}_4$).³⁶ The AdNDP method performs analysis of the first-order reduced density matrix with the purpose of obtaining its local block eigenfunctions with optimal

convergence properties for describing the electron density. The local blocks of the first-order reduced density matrix correspond to the sets of n atoms (from one to all atoms of the molecule) that are tested for the presence of a two-electron object (n -center-two electron ($nc\text{-}2e$) bonds, including core electrons and lone pairs as a special case of $n = 1$) associated with this particular set of n atoms. The AdNDP search starts with core electron pairs and lone pairs (1c-2e), then 2c-2e, 3c-2e, ..., and finally $nc\text{-}2e$ bonds. On each step the density matrix is depleted for the density corresponding to the appropriate bonding elements. The AdNDP procedure can also be applied to specified molecular fragments. This user-directed form of the AdNDP analysis is analogous to the directed search option of the standard NBO code. The recovered $nc\text{-}2e$ bonding elements always correspond to the point-group symmetry of the system after these bonding elements are superimposed onto the molecular frame. For the given n -atomic block those eigenvectors are accepted whose occupation numbers (eigenvalues) exceed the established threshold value and which usually are chosen to be close to 2.00 |el|. Thus, Lewis' idea of an electronic pair as the essential element of bonding is preserved. We consider a molecule as being aromatic if a delocalized bonding is encountered in a planar cyclic system by means of the AdNDP analysis and the number of electrons occupying the delocalized bonds satisfies the $4n + 2$ rule. The AdNDP calculations were performed at the B3LYP level of theory using LanL2DZ (Mo, Sb) and 6-31G* (P, As, C, H) basis sets. All calculations were done using the Gaussian 09 software package.³⁷ Pictures of molecular structures, molecular orbitals, and chemical bonds were made using MOLEKEL 5.4.0.8.³⁸

RESULTS AND DISCUSSION

Our geometry optimization and follow-up frequency calculations of the model $\text{CpMoE}_6\text{MoCp}$ ($E = \text{P, As, Sb}$) complexes

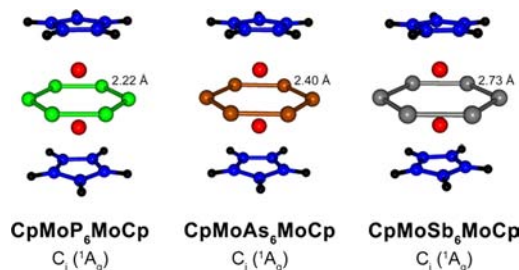


Figure 3. Optimized structures, point group symmetry, spectroscopic states, and bond lengths of the middle-deck fragments in the triple-decker sandwich complexes.

confirm that the C_1 structure (shown in Figure 3) is an energy minimum and E_6 fragments are planar for all practical purposes.

The calculated phosphorus–phosphorus bond length $R(\text{P}–\text{P})$ in the P_6 fragment of the $\text{CpMoP}_6\text{MoCp}$ complex, $R(\text{P}–\text{P}) = 2.22 \text{ \AA}$, is very close to the experimentally measured $R(\text{P}–\text{P}) = 2.17 \text{ \AA}$, but it is a little bit longer than an optimized $R(\text{P}–\text{P}) = 2.13 \text{ \AA}$ of the isolated D_{6h} structure P_6 . Similarly, the calculated $R(\text{As}–\text{As}) = 2.40 \text{ \AA}$ in the As_6 fragment is somewhat longer than $R(\text{As}–\text{As}) = 2.33 \text{ \AA}$ in the isolated D_{6h} As_6 structure. Surprisingly, the optimized $R(\text{Sb}–\text{Sb}) = 2.73 \text{ \AA}$ in the Sb_6 fragment of the $\text{CpMoSb}_6\text{MoCp}$ complex was found to be shorter than $R(\text{Sb}–\text{Sb}) = 2.79 \text{ \AA}$ in the corresponding isolated D_{6h} structure.

As mentioned above, the canonical LUMO of the P_6 ring is responsible for the PJT distortion in this structure due to mixing with the HOMO-1 (Figure 2).

From our molecular orbital analysis (Figure 4) one can see that upon complex formation the molecular orbital (LUMO) corresponding to the empty one in the isolated P_6 structure is now occupied in the triple-decker complex (HOMO-5).

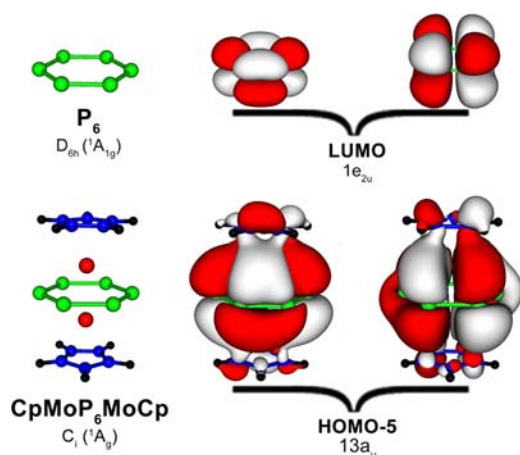


Figure 4. One-to-one correspondence of unoccupied canonical molecular orbitals of P_6 (D_{6h} , $1A_{1g}$) to those of $CpMoP_6MoCp$ (C_i , $1A_g$), where occupation in the latter results in suppression of the PJT effect.

Therefore, to suppress the PJT effect, all unoccupied orbitals connected with its occurrence in the planar P_6 must be occupied in the resultant $CpMoP_6MoCp$ sandwich complex. Using similar analysis for $CpMoAs_6MoCp$ and $CpMoSb_6MoCp$, it was found that the same mechanism is responsible for killing the PJT effect in both complexes, though we do not exclude some influence from the first mechanism.

In order to analyze chemical bonding in the studied triple-decker complexes we initially performed the general AdNDP search for lone pairs and two-center-two-electron (2c-2e) bonds in the whole $CpMoP_6MoCp$ complex. After depleting the overall density for the lone pairs and 2c-2e bonds, we then performed a user-directed search of chemical bonding on each of the fragments ($C_5H_5^-$, P_6 , MoP_6Mo) of the sandwich complex separately. The results of this analysis are shown in Figure 5. Core electrons are omitted from the discussion.

As expected, AdNDP analysis revealed the presence of five 2c-2e C–C σ bonds with occupation numbers (ON) equal to 1.97 |el and five 2c-2e C–H σ bonds (ON = 1.98 |el) for every $C_5H_5^-$ units, one lone pair on every phosphorus atom (not shown in Figure 5), and one direct 2c-2e σ bond (ON = 2.00 |el) between two Mo atoms.

Direct AdNDP search on each $C_5H_5^-$ unit recovered three 5c-2e π bonds (ON = 1.97 – 1.99 |el), which are responsible for the π aromaticity of these fragments. Because of high occupation numbers of π bonds in our direct search on $C_5H_5^-$, it is clear that they do not participate in the π -type back-donation to Mo atoms. Thus, bonding between two $C_5H_5^-$ units and two Mo atoms in the analyzed complex has a significant ionic contribution. The AdNDP search revealed six 2c-2e P–P σ bonds (ON = 1.73 |el) for the planar P_6 unit. Such deviation from an absolute ON = 2.00 |el implies that these 2c-2e P–P σ bonds are delocalized over a larger number of atoms. However, occupation numbers of 1.73 |el are large enough and therefore acceptable for the picture of our qualitative analysis. There are also seven bonds of different types on the fragment which comprises the P_6 unit and two Mo atoms (MoP_6Mo). Three bonds shown in Figure 5h are primarily 6c-2e (excluding negligible antibonding interactions between P_6 and Mo atoms) π bonds (with occupation numbers lying within the 1.90–2.00 |el range), and they are in charge of the π aromaticity in the P_6 fragment.

Another four bonds with ON = 1.94 |el (shown in Figure 5i) are responsible for the covalent bonding between Mo and P_6 through the δ -type M \rightarrow L back-donation mechanism. These bonds are formed by interactions of occupied $d_{x^2-y^2}$ and d_{xy} atomic orbitals of the Mo atom with partially antibonding π -molecular orbitals of P_6 . An occupation of partially antibonding π orbitals is responsible for the elongation of P–P bond lengths upon complexation. AdNDP analysis of chemical bonding in the $CpMoAs_6MoCp$ and $CpMoSb_6MoCp$ complexes revealed similar chemical bonding patterns as in $CpMoP_6MoCp$. The δ -type M \rightarrow L back-donation mechanism was previously described by Rayon and Frenking for bis(benzene)chromium³⁹ as well as Diaconescu et al. for an inverted (μ - C_6H_6)[U-(NH₂)₂]₂ sandwich complex.⁴⁰

CONCLUSIONS

Quantum chemical calculations of the $CpMoE_6MoCp$ (E = P, As, Sb) triple-decker sandwich complexes showed that E_6 fragments in the central decks of the complexes are planar. These results agreed with the experimentally observed $\{(\eta^5-Me_5C_5)Mo\}_2(\mu,\eta^6-P_6)$,⁴ $\{(\eta^5-Me_5C_5)W\}_2(\mu,\eta^6-P_6)$, $\{(\eta^5-Me_4EtC_5)V\}_2(\mu,\eta^6-P_6)$,⁴¹ and $\{(\eta^5-Me_4EtC_5)Mo\}_2(\mu,\eta^6-As_6)$ ⁷ triple-decker sandwich complexes. We are not aware of any experimental data on the decker complexes with Sb_6 fragment. Thus, we only made a theoretical prediction of the existence of the planar *cyclo*- Sb_6 as the central deck.

Analysis of molecular orbitals involved in vibrational coupling showed that filling the intervenient molecular orbitals with electron pairs of Mo atoms suppresses the PJT effect in $CpMoE_6MoCp$ (E = P, As, Sb), with the E_6 ring becoming planar (D_{6h}). Thus, complexation may be considered as the second example of suppression of the PJT effect after reaction between Si_6Cl_{12} and a Lewis base (e.g., Cl^-) to give planar [Si_6Cl_{14}]²⁻ dianionic complexes.²⁸

Our AdNDP analysis revealed that bonding between $C_5H_5^-$ units and Mo atoms in the examined triple-decker sandwich complexes is primarily ionic while bonding between Mo atoms and the E_6 fragment is appreciably covalent through the δ -type M \rightarrow L back-donation mechanism.

We believe that suppressing the PJT effect due to the filling unoccupied molecular orbitals during complex formation is not limited to our examples but is a much more common phenomenon in chemistry. We hope that the current work will attract attention to this suppression mechanism which can become a good tool for constructing new materials with desired planar highly symmetric species.

AUTHOR INFORMATION

Corresponding Author

*E-mail: kbogenko@mail.ru (K.V.B.); a.i.boldyrev@usu.edu (A.I.B.).

Notes

The authors declare no competing financial interest.

ACKNOWLEDGMENTS

The National Science Foundation (Grant CHE-1057746) supported this work. Cluster time and other computational resources from the Center for High Performance Computing at Utah State University are gratefully acknowledged. The computational resources of the 64 node Wasatch cluster were funded by the National Institute of Food and Agriculture, U.S.

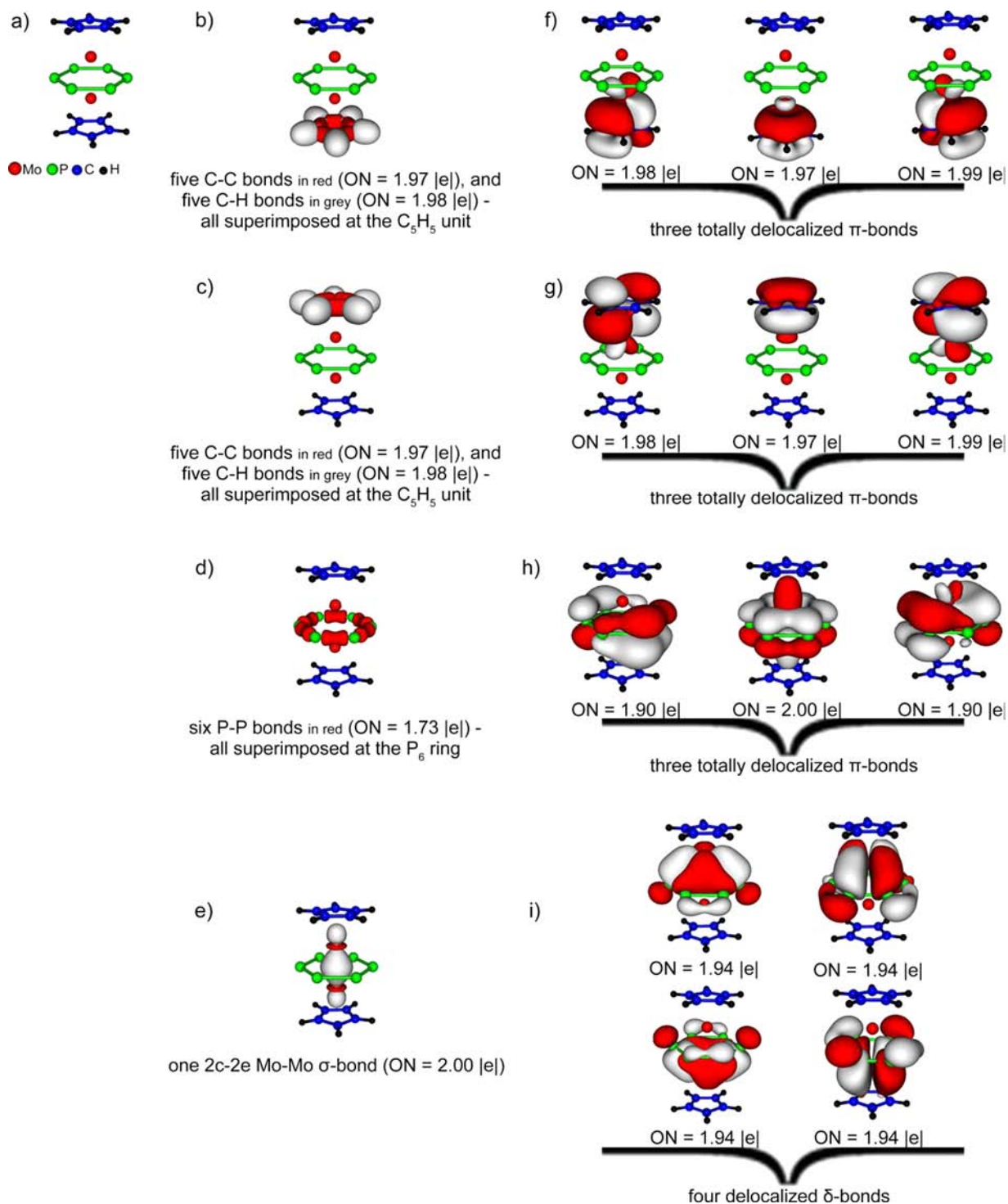


Figure 5. Chemical bonding picture of the CpMoP₆MoCp triple-decker sandwich complex: (a) obtained by the AdNDP method, (b and c) σ bonds recovered on the C₅H₅⁻ units, (d) σ bonds recovered on the P₆ unit, (e) direct Mo–Mo σ bond, (f and g) π bonds recovered on the C₅H₅⁻ units, (h) π bonds recovered on the MoP₆Mo fragment, and (i) δ bonds recovered on the MoP₆Mo fragment.

Department of Agriculture, through the High Performance Computing Utah grant.

REFERENCES

- (1) Gutman, I.; Potgieter, J. H. *J. Chem. Educ.* **1994**, *71*, 222.
- (2) Nagendrappa, G. *Resonance*; The Indian Academy of Sciences: Bangalore, India, May 2001, p 74.
- (3) Dinadayalane, T. C.; Priyakumar, U. D.; Sastry, G. N. *J. Phys. Chem. A* **2004**, *108*, 11433.

- (4) Scherer, O. J.; Sitzmann, H.; Wolmershauser, G. *Angew. Chem., Int. Ed.* **1985**, *24*, 351.
- (5) Scherer, O. J. *Angew. Chem., Int. Ed.* **2000**, *39*, 1029.
- (6) Hiberty, P. C.; Volatron, F. *Heteroat. Chem.* **2007**, *18*, 129.
- (7) Scherer, O. J.; Sitzmann, H.; Wolmershauser, G. *Angew. Chem., Int. Ed.* **1989**, *28*, 212.
- (8) Jemmis, E. D.; Reddy, A. C. *Organometallics* **1988**, *7*, 1561–1564.
- (9) Reddy, A. C.; Jemmis, E. D. *Organometallics* **1992**, *11*, 3894–3900.

- (10) Rani, D. U.; Prasad, D. L. V. K.; Nixon, J. F.; Jemmis, E. D. J. *Comput. Chem.* **2007**, *28*, 310.
- (11) Nguyen, M. T.; Hegarty, A. F. J. *Chem. Soc. Chem. Comm.* **1986**, 383.
- (12) Jones, R. O.; Hohl, D. J. *J. Chem. Phys.* **1990**, *92*, 6710.
- (13) Jones, R. O.; Seiferd, G. J. *J. Chem. Phys.* **1992**, *96*, 7564.
- (14) Warren, D. S.; Gimarc, B. M. *J. Am. Chem. Soc.* **1992**, *114*, 5378.
- (15) Kobayashi, K.; Miura, H.; Nagase, S. *J. Mol. Struct.: THEOCHEM.* **1994**, *69*, 311.
- (16) Gimarc, B. M.; Zhao, M. *Coord. Chem. Rev.* **1997**, *158*, 385.
- (17) Haeser, M.; Schneider, U.; Alhrichs, R. *J. Am. Chem. Soc.* **1992**, *114*, 9551.
- (18) Ballone, P.; Jones, R. O. *J. Chem. Phys.* **1994**, *100*, 4941.
- (19) Haeser, M.; Treutler, O. *J. Chem. Phys.* **1995**, *102*, 3703.
- (20) Galeev, T. R.; Boldyrev, A. I. *Phys. Chem. Chem. Phys.* **2011**, *13*, 20549.
- (21) Opik, U.; Pryce, M. H. L. *Proc. R. Soc. London A* **1957**, *238*, 425.
- (22) Bersuker, I. B. *Phys. Lett. A* **1966**, *20*, 589.
- (23) Bersuker, I. B. *Chem. Rev.* **2001**, *101*, 1067.
- (24) Bersuker, I. B. In *The Jahn-Teller Effect*; Cambridge University Press: Cambridge, U.K., 2006.
- (25) Boggs, J. E.; Polinger, V. Z. In *The Jahn-Teller Effect and Beyond: Selected Works of Isaac Bersuker with Commentaries*; The Academy of Sciences of Moldova: Chisnau, Moldova, 2008.
- (26) Bersuker, I. B.; Stavrov, S. S. *Coord. Chem. Rev.* **1988**, *88*, 1–68.
- (27) Sergeeva, A. P.; Boldyrev, A. I. *Organometallics* **2010**, *29*, 3951.
- (28) Pokhodnya, K.; Olson, C.; Dai, X.; Schulz, D. L.; Boudjouk, P.; Sergeeva, A. P.; Boldyrev, A. I. *J. Chem. Phys.* **2011**, *134*, 014105.
- (29) Becke, A. D. *J. Chem. Phys.* **1993**, *98*, 5648.
- (30) Vosko, S. H.; Wilk, L.; Nusair, M. *Can. J. Phys.* **1980**, *58*, 1200.
- (31) Lee, C.; Yang, W.; Parr, R. G. *Phys. Rev. B: Condens. Matter* **1988**, *37*, 785.
- (32) Hay, P. J.; Wadt, W. R. *J. Chem. Phys.* **1985**, *82*, 299.
- (33) Zubarev, D. Yu.; Boldyrev, A. I. *Phys. Chem. Chem. Phys.* **2008**, *10*, 5207.
- (34) (a) Zubarev, D. Yu.; Boldyrev, A. I. *J. Org. Chem.* **2008**, *73*, 9251. (b) Popov, I. A.; Boldyrev, A. I. *Eur. J. Org. Chem.* **2012**, 3485.
- (35) Zubarev, D. Yu.; Boldyrev, A. I. *J. Phys. Chem.* **2009**, *13*, 866.
- (36) Sergeeva, A. P.; Boldyrev, A. I. *Phys. Chem. Chem. Phys.* **2010**, *12*, 12050–12054.
- (37) Frisch, M. J.; Trucks, G. W.; Schlegel, H. B.; Scuseria, G. E.; Robb, M. A.; Cheeseman, J. R.; Scalmani, G.; Barone, V.; Mennucci, B.; Petersson, G. A.; Nakatsuji, H.; Caricato, M.; Li, X.; Hratchian, H. P.; Izmaylov, A. F.; Bloino, J.; Zheng, G.; Sonnenberg, J. L.; Hada, M.; Ehara, M.; Toyota, K.; Fukuda, R.; Hasegawa, J.; Ishida, M.; Nakajima, T.; Honda, Y.; Kitao, O.; Nakai, H.; Vreven, T.; Montgomery, J. A., Jr.; Peralta, J. E.; Ogliaro, F.; Bearpark, M.; Heyd, J. J.; Brothers, E.; Kudin, K. N.; Staroverov, V. N.; Kobayashi, R.; Normand, J.; Raghavachari, K.; Rendell, A.; Burant, J. C.; Iyengar, S. S.; Tomasi, J.; Cossi, M.; Rega, N.; Millam, N. J.; Klene, M.; Knox, J. E.; Cross, J. B.; Bakken, V.; Adamo, C.; Jaramillo, J.; Gomperts, R.; Stratmann, R. E.; Yazyev, O.; Austin, A. J.; Cammi, R.; Pomelli, C.; Ochterski, J. W.; Martin, R. L.; Morokuma, K.; Zakrzewski, V. G.; Voth, G. A.; Salvador, P.; Dannenberg, J. J.; Dapprich, S.; Daniels, A. D.; Farkas, O.; Foresman, J. B.; Ortiz, J. V.; Cioslowski, J.; Fox, D. J. *Gaussian 09*, Revision B.01; Gaussian, Inc.: Wallingford, CT, 2010.
- (38) Varetto, U. *Molekel*, version 5.4.0.8; Swiss National Supercomputing Centre: Manno, Switzerland, 2009.
- (39) Rayon, V. M.; Frenking, G. *Organometallics* **2003**, *22*, 3304.
- (40) Diaconescu, P. L.; Arnold, P. L.; Baker, T. A.; Mendiola, D. J.; Cummins, C. C. *J. Am. Chem. Soc.* **2000**, *122*, 6108.
- (41) Scherer, O. J.; Schwalb, J.; Swarowsky, H.; Wolmershauser, G.; Kaim, W.; Gross, R. *Chem. Ber.* **1988**, *121*, 443–449.